Vol.2,No.1,2
Winter&Spring,1991

CLINOPYROXENE COMPOSITION AND GENESIS OF BASALTS FROM COLOURED SERIES AND EXOTIC BLOCKS IN THE NEYRIZ AREA (SOUTHERN IRAN): A COMPARISON WITH HAYBI COMPLEX OF OMAN

M. Arvin

Department of Geology, Faculty of Science, University of Kerman, Kerman, Islamic Republic of Iran

Abstract

The pyroxene composition of basaltic rocks from the Coloured Series and Exotic blocks in the Neyriz area are discussed. Comparison has been made with equivalent rocks from Oman. The clinopyroxene compositions are in cognation with trace and rare-earth element analyses which definately confirm the occurrence of three different trends in basic lavas: 1-Depleted tholeiite, 2-Transitional basalt, 3-Alkali basalt. The alkali basalts are considered to be generated by the same processes that produce tholeiitic liquids but are thought to have had a different fractionation history.

Introduction

The Neyriz area lies in the south-eastern part of the Zagros ranges of southern Iran. On the basis of field observation and on petrological grounds, the Neyriz area has been divided into three different structural units; 1-Coloured Series (Hassan-Abad Complex), 2-Ophiolite Complex, 3-Exotic blocks [1]. The Coloured Series is composed mainly of spilite (both as lava flows and pillow lavas), keratophyres, and ignimbrites and more rarely alkaline gabbros, porphyrites, cherts, sandstones and Late-Cretaceous limestones. Tertiary fossiliferous limestones and conglomerates also occur along steep faults. This unit has suffered some imbrication but many internal contacts are undisturbed and the original relation between lavas and sediments are preserved. The Exotic blocks are similar to the Coloured Series, except that there are some differences in the proportion of the sediments to volcanic rocks, the type of volcanic rocks, and occasional occurrence of metamorphic rocks, mainly quartzite and greenschist. The volcanic rocks have been subjected to burial type metamorphism with new minerals replacing the original igneous assemblages. Since composition of pyroxene survives unchanged in rocks which have undergone low-grade metamorphism, clinopyroxene chemistry has been used as a means of reconstructing the paleo-tectonic environment of extrusion and determining the parental magma types [2,3,4,5].

Keywords: Pyroxene, Alkali Basalt, Depleted Tholeiite

Petrography

Volcanic rocks of the Coloured Series and Exotic blocks (Fig.1) characteristically retain their primary igneous textures although alteration has transformed them into spilites and keratophyres. They are typical of rocks which have undergone low-grade metamorphism [6,7].

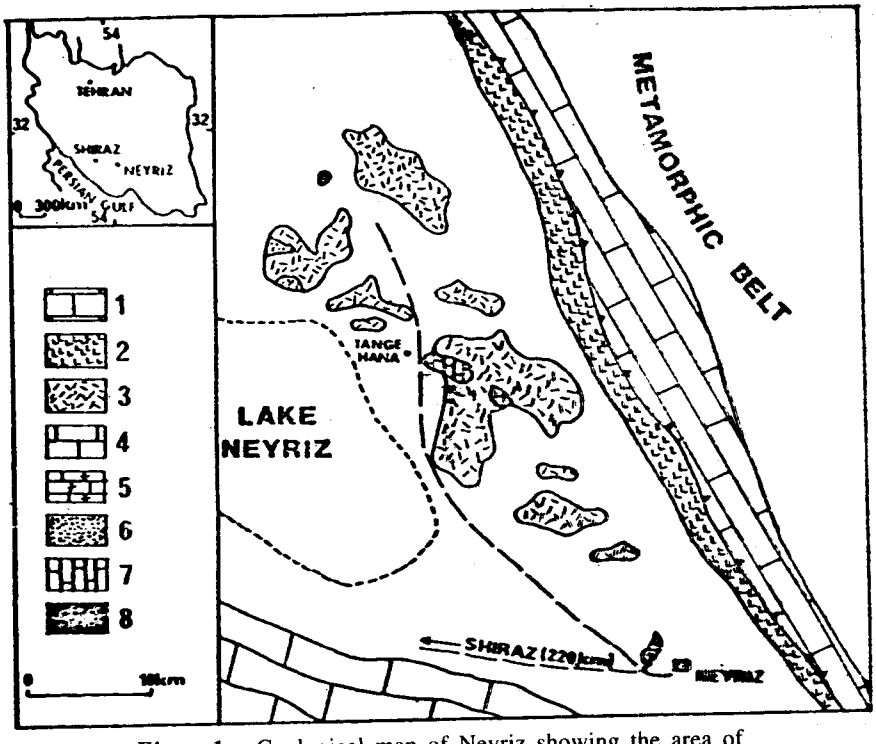

Fig. 1 Geological map of Neyriz showing the area of research (based on Geological map of Iran sheet No. 5. published by NIOC). 1=Main Zagros Thrust. 2=Coloured Series. 3=Ophiolite Complex. 4=Zagros Folded belt. 5= Neyriz Exotic block. 6=Pichegun Exotic block. 7=Tange-Hana marble. 8=Salt plug.

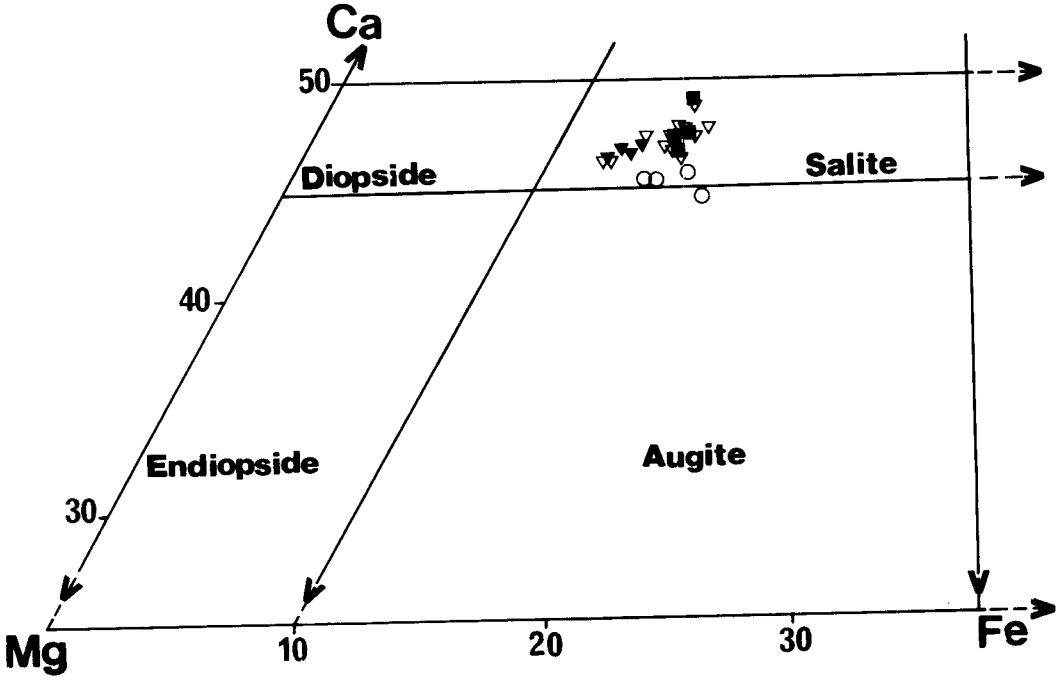

Fig 2. Ca-Fe-Mg diagram for clinopyroxenes of Neyriz alkali basalts in the Coloured Series and the Exotic block units. ■ sample 4-2, ∇ sample 1Ø-2, ▼ sample 47-1, O sample 113-1.

Attention is mainly focused on basic igneous rocks. The spilite is used here for rocks analogus to basalts in their mode of occurrence and texture but consisting largely of low-temperature metamorphic facies minerals such as albite, pumpellyite, epidote and calcite. They occur as flows and pillow lavas and are often vesicular and amygdaloidal. Plagioclase occurs as lath-shaped crystals, groundmass microlites and phenocrysts, typically extensively albitised. Optical determinations of pale green clinopyroxene indicate augite compositions. Porphyritic and glomeroporphyritic textures, defined mainly by phenocrysts of plagioclase and pyroxene are recognized. The groundmass is generally strongly altered although variolitic, pilotaxitic, fluidic and subophitic textures are recognisable. Amygdals are common and mainly filled by calcite and chlorite. The spilites have been subjected to burial type metamorphism and mineral assemblages of the prehnite-pumpellyite facies have been recognized. Alkali basalts occur as small outcrops in an Exotic block a few km north of Neyriz. They contain diopside and kaersutite phenocrysts in a glassy matrix containing clinopyroxene and plagioclase (An_{42}) with pilotaxitic and fluidal textures. Calcite-filled amygdales are characteristic.

Composition of clinopyroxene

A-Alkali basalt

Twenty-four microprobe analyses of clinopyroxenes from four alkali basalts are given in Table 1, and are plotted on part of the pyroxene quadrilateral in Figure 2. All pyroxenes are Ca-rich and fall in, or close to, the salite field (one falls in the augite field). No zoning was detected with respect to Ca-Fe-Mg. The average of Al_2O_3 in clinopyroxenes varies between 3.56-6.03, which corresponds to an average SiO_2 of 49.06-48.17. These differences in Al_2O_3 and SiO_2 content can be explained by a varying degree of differentiation. According to LeBass[8], with differentiation Si increases in non-alkaline and normal alkaline magmas, and the percentage of Al going into tetrahedral coordination decreases. He showed that Al and Ti contents in alkaline

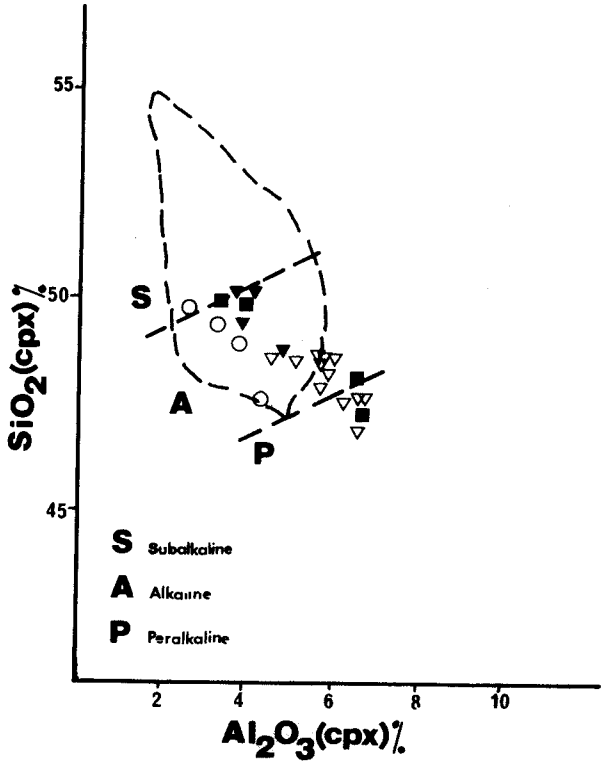

Fig.3 SiO_2 versus Al_2O_3 plot for clinopyroxenes from Neyriz alkali basalts in the Coloured Series and the Exotic block units. After LeBas (1962). Nisbet and Pearce (1977). Symbols as in Fig.2.

clinopyroxene are higher than in the tholeiitic clinopyroxene. The Neyriz alkali basalt clinopyroxenes show a higher Ti content than Neyriz depleted tholeiite clinopyroxenes, although there is some overlap of Al content between the two series. Gibb [9] pointed out that a factor of such degree of fractionation of the parental magma and conditions of crystallization can lead to large overlaps in the composition of pyroxenes from different magma types. The Neyriz alkali basalt pyroxenes plot within the alkaline and peralkaline fields on an Al_2O_3-SiO_2 diagram (Fig. 3).

Nisbet and Pearce [5] used a discriminant method to deduce tectonic setting using analyses from pyroxenes in basaltic rocks. This has the advantage that problems of chemical mobility are reduced but the disadvantage that the discrimination is not as effective as that using

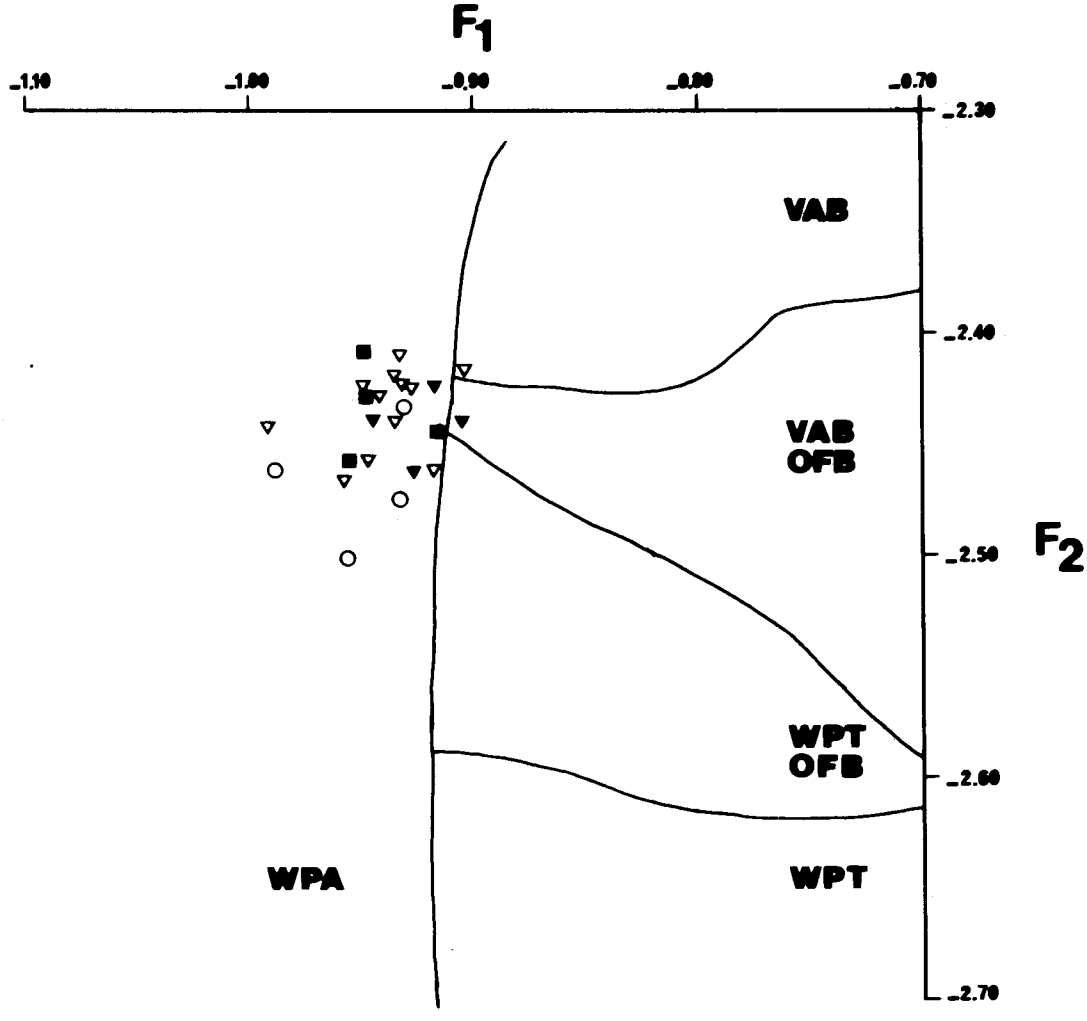

Fig.4 Plot of discriminant functions F_1 versus F_2 for clinopyroxene compositions from Neyriz alkali basalt in the Coloured Series and the Exotic block units. After Nisbet and Pearce, 1977. Symbols as in Fig. 2 VAB=Volcanic arc basalts, OFB=Ocean floor basalts, WPT=Within plate tholeiitic basalts, WPA=Within plate alaklic basalts. F_1 and F_2 are a set of scaled eigenvectors which are calculated based on the result of discriminant analysis and certain coefficient numbers).

immobile trace elements. Figure 4 shows a plot of the discriminant functions F_1 and F_2 [5] for the Neyriz alkali basalt pyroxene analyses, where they plot in the WPA field, and clearly supports the conclusion using trace element analyses for the Neyriz alkali basalt [10]. Pyroxenes from alkali volcanic rocks in Haybi complex also plot in the field of "within-plate" alkaline magmas, on the discriminant function diagram [11].

B-Depleted tholeiite

Eleven microprobe analyses of clinopyroxenes from two depleted tholeiites are given in Table 2 and are plotted on part of the pyroxene quadrilateral in Figure 5. They mainly plot in the diopside and augite fileds. No zoning was detected with respect to Ca-Fe-Mg. The pyroxenes plot mainly in the non-alkaline field on SiO_2-Al_2O_3 diagram (Fig. 6). The plot of discrimination function F_1 and F_2 (Fig.7) for the pyroxene analyses, which plot in VAB+OFB field, clearly supports the conclusion using trace element analyses for the Neyriz depleted tholeiites [10]. Pyroxenes from depleted tholeiites in the Haybi complex also plot in the tholeiite half of the discriminant diagram [11].

C=Transitional basalt

Nine microprobe analyses of clinopyroxenes from a transitional basalt are given in Table 3. They fall in the augite field on the Ca-Fe-Mg component diagram (Fig. 5). No zoning was detected with respect to Ca-Fe-Mg. The majority of pyroxenes fall in the alkaline field on SiO_2-Al_2O_3 diagram (Fig. 6), however their relatively low Ti in comparison with Neyriz alkali basalt, and low Al are closer to tholeiitic rather than alkaline pyroxene. On the discriminant diagram (Fig. 7) they fall mainly in VAB+0FB which is in contrast with the results of their trace element analyses [10]. However, in view of the transitional nature of the basalt, the above diagram should be treated with caution, since there is no discussion of the use of the above diagrams for the pyroxene of transitional basalts in the literature. Searle et al. [11] did not apply the above diagrams to their transitional basalts in the Haybi complex.

Conclusion

Three different types of basalts (alkali, transitional, and depleted tholeiite) in the Coloured Series and Exotic block units have distinctive trace element chemistries and REE patterns (10). This is also reflected in their mineralogy, especially the clinopyroxene compositions.

It has been suggested by many authors [12,13,14] that basaltic magmas are in equilibrium with their major phases at low pressures and, if generated at depth, may have suffered extensive fractionation on their way to the surface to maintain equilibrium. The contention, based on this evidence, is that not only is the depth of magma generation important but also the rate at which the liquid moves toward the surface and the pressure regimes in which it fractionates. Cann [15] suggested that beneath the oceanic spreading axes (regions of exceptionally high geothermal gradient) the earth's mantle is partially molten at a depth of less than 10 km. In this model, the Neyriz depleted tholeiite magma would be produced high in the mantle in a very low pressure environment.

Therefore, the tholeiitic magma would be generated by Cann as a primary liquid. However, it has been argued by Gass et al. [16] that as a high heat flow is restricted to narrow linear zones, it is caused by magmatic activity and is not the cause of it. They consider that melting occurs much deeper in the mantle and the rise of liquid beneath spreading axes is the cause of high heat flow. O'Hara [17] suggested that all basalts are fractionated products of picritic primary liquid which is generated at some depth in the mantle. Tholeiitic melts are evolved liquids which are produced from a picritic partial melt by olivine fractionation during magma ascent. This view has become more widely accepted and the main arguments are summarised for it by Elthon [18].

Using O'Hara's model, the Neyriz depleted tholeiite is an evolved liquid generated in the following way: a primary picritic magma was generated at c. 100km and ascended rapidly to the surface, crystallising only olivine. A depleted tholeiite was produced from this fractionated liquid after plagioclase crystallisation at a high level in the mantle. However, the Neyriz tholeiites are very depleted in incompatible trace elements and LREE compared to MORB [10]. This depletion can be explained if the source mantle of the picritic magma was already depleted by an earlier melting event. This is often considered to be characteristic of island arc regions because the mantle of island arc regions should be depleted by earlier melting at mid-oceanic ridge. Therefore, the Neyriz depleted tholeiites could be interpreted as island arc tholeiites. However, Duncac and

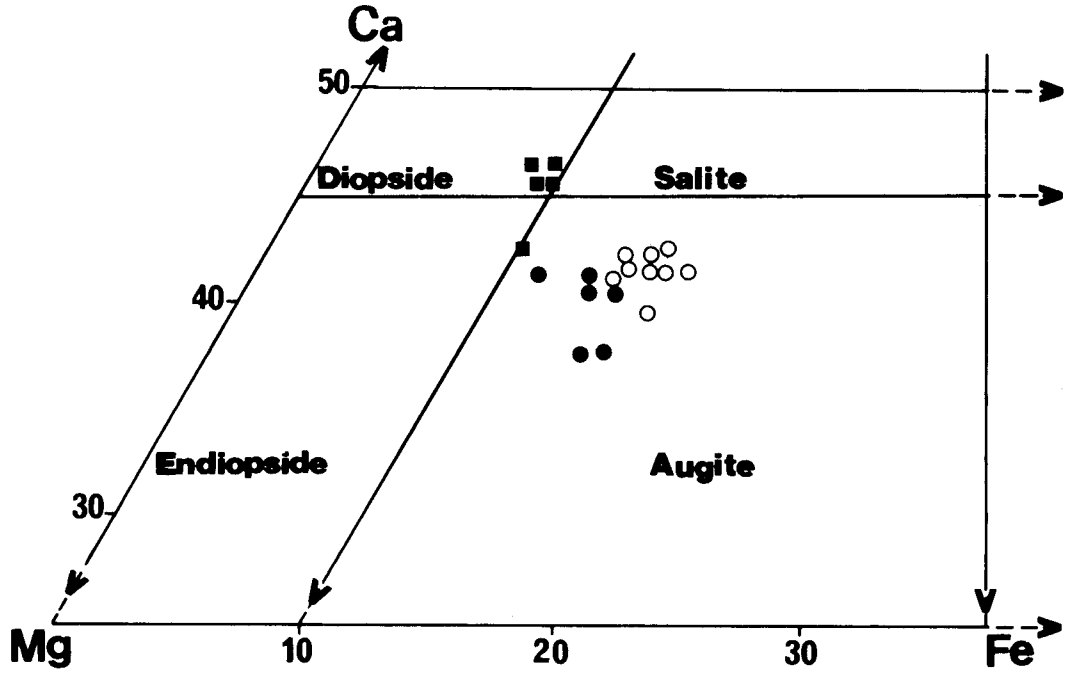

Fig.5 Ca-Fe-Mg diagram of clinopyroxenes from Neyriz depleted tholeiites and transitional basalt in the Coloured Series and the Exotic block units. ■ sample 40-2, ● sample 48-2. o sample 124-1 (transitional basalt).

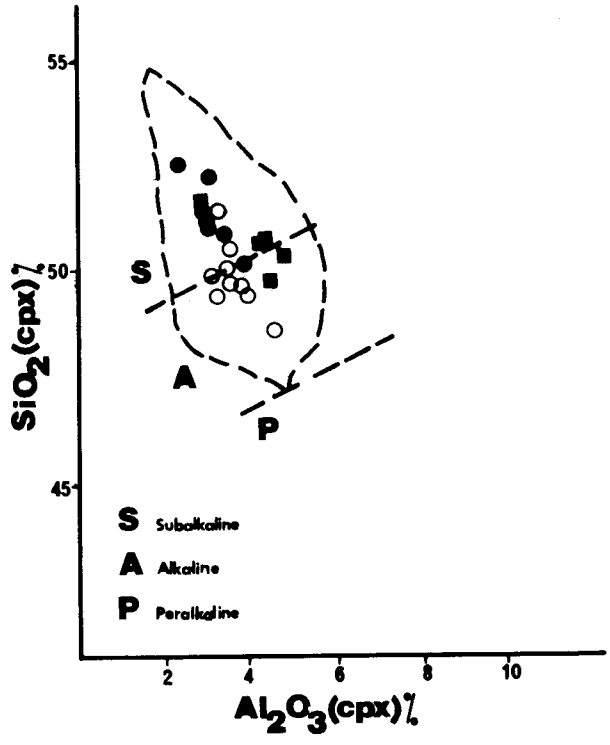

Fig.6 SiO_2 versus Al_2O_3 plot for clinopyroxenes from Neyriz depleted tholeiites and transitional basalt in the Coloured Series and Exotic block units. After LeBas (1962). Nisbet and Pearce (1977). Symbols as in Fig. 5.

Green [19] have suggested that depleted tholeiites can also be produced in normal oceanic areas by a multi-stage melting process in which lherzolite diapirs form as a result of partial melting deep in the mantle, rise and then second stage melts are formed at shallow depth (25km). In this case, depleted tholeiites are formed, but do not indicate an island arc origin, despite their geochemical similarities. The depletion will be a feature of any multi-stage melting process, wherever it occurs.

Two chief hypotheses have been suggested for the generation of the alkali basalts. Kushiro [20] considered alkali basalts to be primary liquids but generated at higher pressures (and therefore greater depths) than primary tholeiitic liquids. To be applicable in an area such as Neyriz, where both alkali and tholeiitic basalts occur together, this model would require some major mantle feature, such as a transform fault, to allow the alkali basalt melt to rise to the surface without fractionation. However, tholeiitic magmas are now not generally regaded as primary liquids, nor are alkali basalt magmas. Instead alkali basalts are considered to be generated by the same processes that produced tholeiitic liquids, but to have had a different fractionation history. For example, they could have risen to the surface more slowly to give time for more extensive fractionation than depleted tholeiites. Using this model, transitional basalts are to have formed at some intermediate depth.

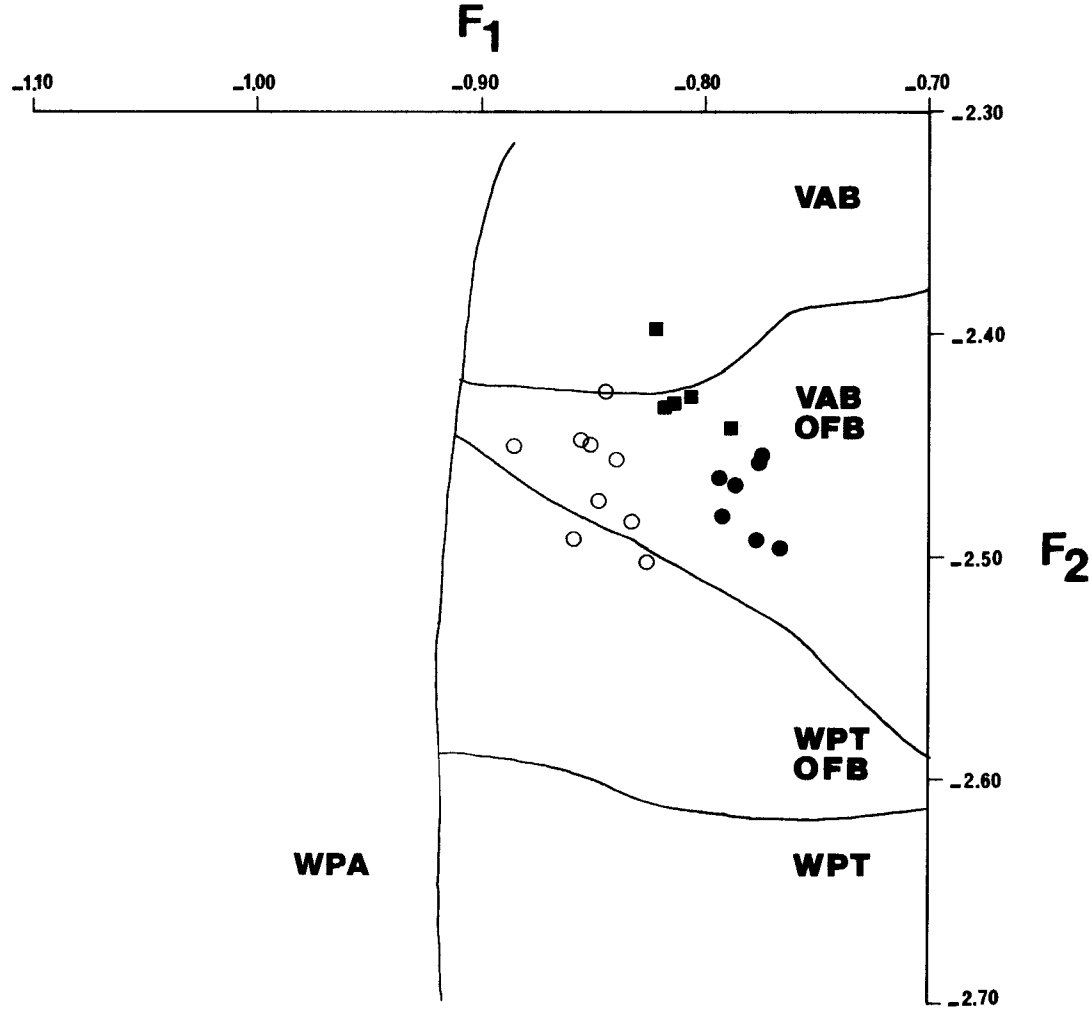

Fig.7 Plot of discriminant functions F_1 versus F_2 for clinopyroxenes compositions from Neyriz depleted tholeiites and transitional basalt in the Coloured Series and Exotic block units. After Nisbet and Pearce. 1977. Symbols as in Fig. 5. Different fields as in Fig. 4

Table 1 Electron Microprobe analyses of calcic clinopyroxenes (Total Fe as FeO)

	10-2	10-2	10-2	10-2	10-2	10-2	10-2	10-2	10-2	10-2	10-2
SiO_2	47.71	46.93	47.94	48.90	48.38	47.65	47.98	47.76	48.72	48.74	48.57
TiO_2	2.04	2.49	2.03	1.56	1.76	1.88	1.81	2.12	1.88	1.91	1.97
Al_2O_3	6.59	6.71	5.99	4.66	5.88	6.50	5.88	6.77	5.82	5.88	5.39
FeO	8.80	8.76	8.56	8.26	7.26	8.68	8.43	8.42	7.54	8.41	8.87
MnO	nd	0.19	0.19	0.16	nd	0.15	0.20	nd	nd	0.15	0.27
MgO	12.16	12.09	12.33	12.83	13.92	12.78	12.83	11.92	13.26	12.57	13.04
CaO	21.32	21.83	21.72	21.98	21.50	21.28	21.40	21.70	22.25	22.14	21.78
Na_2O	0.86	1.14	0.91	1.02	0.73	1.03	0.89	0.89	0.91	0.77	0.87
Total	99.48	100.14	99.67	99.37	99.46	99.95	99.41	99.58	100.38	100.57	100.76
Pyroxene ions calculated on a theoretical basis of 0=6 per unit formula											
Si	1.797	1.766	1.805	1.844	1.810	1.788	1.808	1.795	1.812	1.815	1.811
Al^{IV}	0.203	0.234	0.195	0.156	0.190	0.212	0.192	0.205	0.188	0.185	0.189
Total	2.000	2.000	2.000	2.000	2.000	2.000	2.000	2.000	2.000	2.000	2.000
Al^{VI}	0.090	0.064	0.071	0.051	0.068	0.076	0.069	0.095	0.067	0.073	0.048
Ti	0.058	0.070	0.057	0.044	0.050	0.053	0.052	0.060	0.053	0.053	0.055
Fe	0.277	0.276	0.270	0.261	0.226	0.272	0.266	0.265	0.234	0.262	0.276
Mn	nd	0.006	0.006	0.005	nd	0.005	0.007	nd	nd	0.005	0.009
Mg	0.683	0.678	0.692	0.721	0.776	0.715	0.721	0.668	0.735	0.698	0.725
Total	1.108	1.094	1.096	1.082	1.120	1.121	1.115	1.088	1.089	1.091	1.113
Ca	0.860	0.880	0.876	0.888	0.854	0.856	0.864	0.874	0.887	0.883	0.870
Na	0.063	0.083	0.066	0.075	0.053	0.075	0.065	0.065	0.066	0.056	0.063
Total	0.923	0.963	0.942	0.963	0.907	0.931	0.929	0.939	0.953	0.939	0.933
Mg	37.52	36.84	37.55	38.45	41.63	38.79	38.80	36.87	39.67	37.80	38.56
Fe	15.23	15.33	14.92	14.19	12.16	14.76	14.70	14.53	12.50	14.42	15.16
Ca	47.25	47.83	47.53	47.36	46.21	46.45	46.50	48.60	47.82	47.78	46.27

	10-2	4-2	4-2	4-2	4-2
SiO_2	48.75	48.36	50.13	50.04	47.40
TiO_2	1.77	1.72	1.61	1.28	1.97
Al_2O_3	6.26	6.73	3.47	4.15	6.88
FeO	7.13	8.46	9.22	8.79	8.47
MnO	0.18	0.21	0.22	0.20	0.21
MgO	13.91	12.01	12.86	13.02	12.52
CaO	21.77	22.09	22.63	21.71	21.61
Na_2O	0.73	1.11	0.68	0.75	1.13
Total	100.50	100.69	100.82	99.94	100.19

Tabel 1 Continued

	10-2	4-2	4-2	4-2	4-2
Si	1.804	1.801	1.871	1.873	1.776
Al^{IV}	0.196	0.199	0.129	0.127	0.224
Total	2.000	2.000	2.000	2.000	2.000
Al^{VI}	0.077	0.096	0.024	0.056	0.080
Ti	0.049	0.048	0.045	0.036	0.056
Fe	0.221	0.264	0.288	0.275	0.265
Mn	0.006	0.007	0.007	0.006	0.007
Mg	0.767	0.667	0.715	0.726	0.699
Total	1.120	1.082	1.079	1.099	1.107
Ca	0.863	0.882	0.905	0.871	0.868
Na	0.052	0.080	0.049	0.054	0.082
Total	0.915	0.926	0.954	0.925	0.950
Mg	41.35	36.66	37.57	38.71	38.12
Fe	12.18	14.44	14.81	14.52	14.36
Ca	46.47	48.88	47.62	46.77	47.51

	47-1	47-1	47-1	47-1	113-1	113-1	113-1	113-1
SiO_2	48.97	50.35	50.43	49.57	49.98	49.02	47.54	49.72
TiO_2	1.72	1.39	1.38	1.38	1.69	2.32	2.71	1.84
Al_2O_3	4.70	3.63	4.23	3.86	2.60	3.98	4.40	3.26
FeO	8.05	7.75	7.60	7.63	8.76	9.04	9.82	8.80
MnO	0.19	0.27	nd	0.23	0.25	0.29	0.20	nd
MgO	13.45	13.87	14.01	13.84	13.83	13.16	12.91	13.95
CaO	22.29	22.29	22.09	22.10	21.55	21.56	20.88	21.53
Na_2O	0.84	0.72	0.73	0.82	0.55	nd	0.76	0.69
K_2O	nd	nd	nd	nd	nd	nd	nd	nd
Total	100.28	100.27	100.47	99.43	99.21	99.37	99.22	99.79
Si	1.830	1.874	1.867	1.862	1.888	1.849	1.809	1.866
Al^{IV}	0.170	0.126	0.133	0.138	0.112	0.151	0.191	0.134
Total	2.000	2.000	2.000	2.000	2.000	2.000	2.000	2.000
Al^{VI}	0.037	0.033	0.052	0.033	0.004	0.026	0.006	0.010
Ti	0.050	0.039	0.038	0.039	0.048	0.066	0.078	0.052
Fe	0.252	0.241	0.235	0.240	0.277	0.285	0.313	0.276
Mn	0.006	0.009	nd	0.007	0.008	0.009	0.006	nd
Mg	0.749	0.770	0.773	0.775	0.778	0.740	0.732	0.780
Total	1.094	1.092	1.098	1.094	1.115	1.126	1.135	1.118
Ca	0.892	0.889	0.876	0.890	0.872	0.871	0.851	0.866
Na	0.061	0.052	0.052	0.060	0.040	nd	0.056	0.050
K	nd	nd	nd	nd	nd	nd	nd	nd

Tabel 1 Continued

Total	0.953	0.941	0.928	0.950	0.912	0.871	0.907	0.916
Mg	39.36	40.42	41.18	40.74	40.21	38.85	38.49	40.58
Fe	13.30	12.77	12.30	12.70	14.73	15.43	16.77	14.36
Ca	47.34	46.81	46.52	46.56	45.06	45.72	44.74	45.06

Table 2 Electron Microprobe analyses of calcic. clinopyroxenes (Total Fe as FeO)

	40-2	40-2	40-2	40-2	40-2	48-2	48-2	48-2	48-2	48-2	48-2
SiO_2	50.58	50.55	51.44	49.54	50.34	51.09	51.38	52.80	51.21	50.95	51.37
TiO_2	0.69	0.70	0.54	0.90	0.73	0.59	0.52	0.39	0.47	0.50	0.52
Al_2O_3	4.50	4.36	2.97	4.72	5.02	3.37	3.37	2.49	3.71	3.75	3.21
FeO	5.75	5.30	6.66	5.71	5.45	9.60	8.15	6.90	8.48	8.85	9.20
MnO	0.13	0.22	0.15	0.14	0.18	0.34	0.24	0.15	0.18	0.20	0.32
MgO	15.37	15.41	16.44	14.86	15.60	16.21	16.09	17.00	15.67	15.45	16.39
CaO	21.49	21.94	20.43	21.99	22.09	18.45	20.27	20.73	19.58	19.26	18.02
Na_2O	nd	nd	nd	nd	nd	nd	nd	nd	nd	nd	nd
Cr_2O_3	0.54	0.46	0.16	0.37	0.73	nd	nd	nd	nd	nd	nd
Total	99.05	98.94	98.79	98.23	100.14	99.65	100.02	100.46	99.30	98.96	99.03
	Pyroxene ions calculated on a theoretical basis of 0=6 unit formula										
Si	1.877	1.878	1.914	1.860	1.851	1.901	1.900	1.931	1.905	1.904	1.916
Al^{IV}	0.123	0.122	0.086	0.140	0.149	0.099	0.100	0.069	0.095	0.096	0.084
Total	2.000	2.000	2.000	2.000	2.000	2.000	2.000	2.000	2.000	2.000	2.000
Al^{VI}	0.074	0.069	0.044	0.069	0.069	0.049	0.047	0.038	0.068	0.069	0.057
Ti	0.019	0.020	0.015	0.025	0.020	0.017	0.014	0.011	0.013	0.014	0.015
Fe	0.178	0.165	0.207	0.179	0.168	0.299	0.252	0.211	0.264	0.77	0.287
Mn	0.004	0.007	0.005	0.004	0.006	0.011	0.008	0.005	0.006	0.006	0.010
Mg	0.850	0.853	0.912	0.831	0.855	0.899	0.887	0.927	0.869	0.861	0.911
Cr	0.016	0.014	0.005	0.011	0.021	nd	nd	nd	nd	nd	nd
Total	1.141	1.128	1.188	1.119	1.139	1.275	1.208	1.192	1.220		
Ca	0.855	0.873	0.815	0.885	0.870	0.736	0.803	0.812	0.781	0.771	0.720
Na	nd	nd	nd	nd	nd	nd	nd	nd	nd	nd	nd
Total	0.855	0.873	0.815	0.885	0.870	0.736	0.803	0.812	0.781	0.771	0.720
Mg	45.45	45.21	47.03	44.15	45.02	46.22	45.49	47.42	45.26	44.96	47.50
Fe	9.10	8.51	10.93	9.04	9.16	15.94	13.33	11.05	14.06	14.78	14.96
Ca	45.45	46.28	42.03	46.80	45.81	37.84	41.18	41.53	40.68	40.26	37.54

Table 3 Electron Microprobe analyses of calcic clinopyoxenes (Total Fe as FeO)

	124-1	124-1	124-1	124-1	124-1	124-1	124-1	124-1	124-1
SiO_2	50.15	50.22	48.52	49.65	49.78	49.50	50.60	51.49	49.85
TiO_2	1.02	0.89	1.67	1.27	1.41	1.31	1.15	1.00	1.26
Al_2O_3	3.34	3.55	4.74	4.04	3.84	3.45	3.59	3.38	3.66
FeO	8.80	8.35	9.41	9.44	10.79	9.77	10.09	9.09	9.57
MnO	0.29	0.19	0.24	0.19	0.29	0.25	0.15	0.15	0.22
MgO	14.98	15.21	14.12	14.22	14.16	14.67	15.30	15.51	14.04
CaO	19.74	20.23	19.55	19.77	19.60	19.96	19.18	19.77	19.94
Na_2O	0.67	0.75	0.65	nd	nd	nd	0.17	nd	nd
Cr_2O_3	0.27	0.31	0.35	0.20	nd	0.21	0.19	0.22	0.22
Total	99.26	99.61	99.25	98.78	99.87	99.12	100.42	100.61	98.76
Pyroxene ions calculated on a theoretical basis of 0=6 per unit formula									
Si	1.883	1.877	1.830	1.873	1.869	1.868	1.879	1.898	1.883
Al^{IV}	0.117	0.123	0.170	0.127	0.131	0.132	0.121	0.102	0.117
Total	2.000	2.000	2.000	2.000	2.000	2.000	2.000	2.000	2.000
Al^{VI}	0.031	0.033	0.041	0.053	0.039	0.022	0.036	0.045	0.046
Ti	0.029	0.025	0.047	0.036	0.040	0.037	0.032	0.028	0.036
Fe	0.276	0.261	0.297	0.298	0.339	0.308	0.313	0.280	0.302
Mn	0.009	0.006	0.008	0.006	0.009	0.008	0.005	0.005	0.007
Mg	0.838	0.842	0.794	0.800	0.792	0.825	0.847	0.852	0.791
Cr	0.008	0.009	0.010	0.006	nd	0.006	0.006	0.006	0.007
Total	1.191	1.176	1.197	1.199	1.219	1.206	1.239	1.216	1.189
Ca	0.794	0.810	0.790	0.799	0.792	0.807	0.763	0.781	0.807
Na	0.049	0.054	0.048	nd	nd	nd	0.012	nd	nd
Total	0.843	0.864	0.838	0.799	0.792	0.807	0.875	0.781	0.807
Mg	43.67	43.83	42.21	42.55	41.58	42.33	43.98	44.50	41.79
Fe	14.98	14.03	15.79	15.42	17.37	16.27	16.23	14.66	15.87
Ca	41.35	42.14	41.99	42.02	41.05	41.40	39.79	40.84	42.32

References:

1- Arvin, M. Petrology and geochemistry of ophiolites and associated rocks from the Zagros suture, Neyriz, Iran. Ph.D. Theses, Univ. Coll. Lond. 299p (1982).

2- Beccaluva, L., Macciotta, G., Piccardo, G.B., and Zeda, O. Clinopyroxene composition of ophiolite basalt as petrogenetic indicator. *Chem. Geol.* **77,**. 165-182 (1989).

3- Leterrier, J., Maury, R.C., Thonon, P., Girard, D., and Marchal, M. Clinopyroxene composition as a method of identification of the magmatic affinities of paleo-volcanic series. *Earth. Plant. Sci. Lett.* **59.,** 139-154 (1982).

4- Kornprobst, J., Ohnestetter, D., and Ohnestetter, M. Na and Cr contents in clinopyroxenes from peridotites: A possible discriminant between "sub-continental" and "sub-oceanic" mantle. *Earth. Plant. Sci. Lett. 53.*, 241-254 (1981).

5- Nisbet, E.G., and Pearce, J.A. Clinopyroxene composition in mafic lavas from different tectonic settings. *Contrib. Mineral. Petrol.* **63.,** 149-160 (1977).

6- Levi, B. Burial metamorphism of a Cretaceous volcanic sequence, west from Santiago Chile. *Contrib. Mineral. Petrol.* **24.,** 30-49 (1969).

7- Vallance, T.G. Spilites again: Some consequences of the dehydration of basalts. Proc. Linn. Soc. N.S.W. 94., 8-51 (1969).

8- LeBas, M.J. The role of aluminum in igneous clinopyroxenes

with relation to their parentage. *Am. Jour. Sci.* **260.,** 267-288 (1962).

9- Gibb, F.G.F. The zoned clinopyroxenes of the Shiant isles sill, *Scotland. Jour. Petrol.* **14., 203-230 (1973).**

10- Arvin, M. Petrology and geochemistry of ophiolites and associated rocks from the Zagros suture, Neyriz, Iran. Ophiolite. Symposium. Cyprus. in progress (1990).

11- Searle, M.P., Lippard, S.J., Smewing, J.D., and Rex, D.C. Volcanic rocks beneath the Oman mountains and thier significance in the Mesozoic evolution of Tethys. *Q. Jour. Geol. Soc. Lond.* **137.,** 589-604 (1980).

12- O'Hara, M.J. Primary magmas and the origin of basalts. *Scotl. Jour. Geol.* **1.,** 19-40 (1965).

13- O'Hara, M.J. Are ocean floor basalts primary magma nature. *Nature,* 683-686 (1968b).

14- Green, D.H., and Ringwood, D. The genesis of basaltic magmas. *Contr. Mineral. Petrol.* **15.,** 103-190 (1967).

15- Cann, J.R. New model for the structure of the ocean crust. *Nature,* **226:,** 928-930 (1970).

16- Gass, I.G., Mallick, D.I.J., and Cox, K.G. Vlocanic islands of the Red Sea. *O. Jour. Geol. Soc. Lond.* **129.,** 275-310 (1973).

17- O'Hara, M.J. Geochemical evolution during fractional crystallisation of a periodically riffiled magma chamber. *Nature,* **266.,** 503-507 (1977).

18- Elthon, D. High magnesia liquids as the parental magma for ocean floor basalts. *Nature,* **278.,** 514-518 (1979).

19- Duncan, R.A., and Green, D.H. Role of multi-stage melting in the formation of oceanic crust. **Geol. 8.,** 22-26 (1980).

20- Kushiro, I. Partial melting of synthetic and natural peridotites at high pressures. Carnegie Inst. Washington Year Book. 71., 357-362 (1972).